Sensorless Field Oriented Control of SVM Inverter Fed Induction Machine in Field Weakening Region using Sliding Mode Observer

Nisha G.K., *Member, IAENG*, Lakaparampil Z.V., *Member, IEEE* and Ushakumari S.

Abstract— **One of the primary advantages of vector controlled induction machine for high performance application is the capability for easy field weakening and the full utilization of voltage and current rating of the inverter to obtain a wide dynamic speed range. In a sensorless vector controlled induction machine, the speed must be estimated from the system measurements. In the high speed region, the measure of rotor speed and the sensitivity to parameter error of the motor is a problem. Model Reference Adaptive System (MRAS) based techniques are one of the best methods to estimate the rotor speed due to its performances and straight forward stability approach. In this paper, a new robust MRAS scheme based on sliding mode technique to estimate the rotor speed of a sensorless vector controlled induction machine in the field weakening (FW) region is proposed. Further, a space vector pulse width modulated (SVPWM) voltage source inverter is used to feed the induction machine rather than the traditional sinusoidal PWM inverter for the simulation. The drive system with the proposed adaptive mechanism is simulated by MATLAB/Simulink to verify the performance of the technique.**

***Index Terms*—Field weakening, Induction machine, Model reference adaptive system, Sliding mode observer.**

I. Introduction

POWER electronics has greatly expanded the use of induction machine ranges from consumer to automotive applications such as washing machine to traction in power train. These applications require the achievement of high speed while having a high torque value only at low speeds. In order to achieve these requirements, the induction machine is to be operated in field weakening (FW) region, which is above the base speed of the machine. In order to increase the produced torque to a maximum level in the FW region, it is necessary to suitably adjust the machine's magnetic field by maintaining the maximum voltage and maximum current. The loss of torque and power is up to 35% in the case of improperly adjusted machine flux [1].

Manuscript received March 03, 2013.

Nisha G. K. is with the Department of Electrical and Electronics Engineering, College of Engineering, Trivandrum, Kerala, India. (e-mail: nishacharu@gmail.com).

Lakaparampil Z. V. is with the Centre for Development of Advanced Computing (C-DAC), Trivandrum, Kerala, India. (e-mail: zvlakapara@cdactvm.in)

Ushakumari S. is with the Department of Electrical and Electronics Engineering, College of Engineering, Trivandrum, Kerala, India. (e-mail: ushalal2002@gmail.com).

During the past two decades, several research papers were presented in order to achieve the maximum torque capability of the machine in the FW region and suggested various approaches [2]-[17]. The FW approaches can be categorized as: i) variation of stator flux in inverse proportion to the rotor speed ($1/\omega_r$); ii) feed forward reference flux generation on machine equations or machine models and iii) closed loop control of the stator voltage or voltage detection model.

The first approach as presented in [2] and [3], the most frequently used approach in FW control, the flux is established inversely proportional to the motor speed. Although the method is simple, it is justified only when considering the machine a linear magnetic circuit. In real situations, the transition from nominal excitation to FW de-saturates the magnetic circuit. Thus the machine gets overexcited as the optimal balance between the magnetizing and the torque producing current components. The method thus cannot produce maximum output torque for the available current and the full utilization of DC-link voltage.

The second approach, as presented in [4]-[5], relies on the nonlinear equations of machine model and the constraints of voltage and current, which makes it parameter dependent. Thus the method can provide accurate results only if magnetic saturation is considered with known machine parameters of sufficient accuracy.

The third approach as described in [6]-[17], maximum available inverter voltage is utilized to produce maximum torque in FW region when the excitation level is adjusted by closed loop control of the machine voltage. Although it is not dependent on motor parameters and DC link voltage, demands an additional outer loop which is to be tuned and requires intensive computation.

On comparing the above three approaches, the method based on machine model seems to be a more practical approach with reasonable results. The major problem of the machine model approach in the FW region is the substantial variation of magnetizing inductance which is considered constant in the base speed range. In the FW region, the rotor flux is getting reduced to below its rated value due to the increase of rotor speed than the base speed. The variable level of the main flux saturation in the machine causes the variation of magnetic inductance [18]. Therefore, in model based approach, accurate speed estimation is possible only if the speed estimation algorithm is modified to account the variation of magnetic inductance in the FW region. In the literature, modeling of magnetizing inductance of induction machine has been discussed extensively in [19]-[22].

ISBN: 978-988-19252-8-2
ISSN: 2078-0958 (Print); ISSN: 2078-0966 (Online)

In [23], a mathematical model for speed estimation of sensorless vector control of SVPWM inverter fed induction machine using MRAS scheme based on sliding mode observer which combines sliding mode theory and Lyapunov's stability theory has been presented with simulation results. In particular, aim of this paper is to extend the simulation carried out in [23] with theoretical modification for a sensorless vector controlled induction machine in FW region, such that the machine can be operated in wide speed range.

The paper is organized as follows. Section II provides the dynamic model of induction machine. Section III presents the field weakening control of induction machine. Section IV explains SVPWM based three phase inverter. Section V explains theory of sliding mode MRAS speed observer with stability criteria. Section VI explains the simulation and Section VII discusses the simulation results generated by MATLAB/Simulink.

II. Dynamic Model of Induction Machine

The principle of vector control of AC machine can be controlled to give dynamic performance comparable to the separately excited DC motor. Independent control of motor flux and torque can be obtained by this method, it is possible by connecting coordinate system with rotor flux vector. Fig. 1 shows the vector diagram of induction motor in stationary *α-β* and rotating *d-q* coordinates. The reference frame *d-q* is rotating with the angular speed equal to rotor flux vector angular speed ω_e. Induction motor model equation in *d-q* reference frame is written as follows:

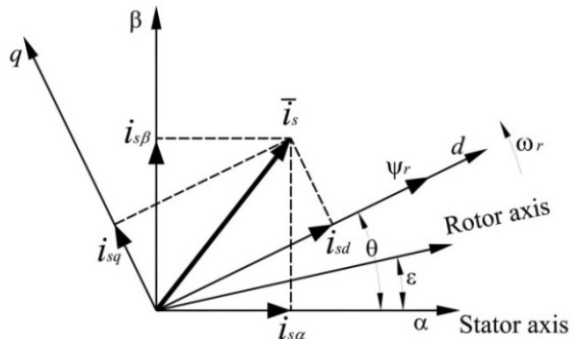

Fig. 1. Phasor diagram of field oriented drive system

$$\vec{V}_s(t)e^{-j\theta} = R_s\vec{i}_s e^{-j\theta} + L_s\frac{d\vec{i}_s}{dt}e^{-j\theta} + L_m\frac{d(\vec{i}_r e^{j\varepsilon})}{dt}e^{-j\theta} \tag{1}$$

$$0 = R_r\vec{i}_r e^{j(\varepsilon-\theta)} + L_r\frac{d\vec{i}_r}{dt}e^{j(\varepsilon-\theta)} + L_m\frac{d(\vec{i}_s e^{-j\varepsilon})}{dt}e^{j(\varepsilon-\theta)} \tag{2}$$

$$\frac{d\omega_r}{dt} = \frac{T_d(t)-T_L(t)}{J} = \frac{1}{J}\left(\frac{2}{3}\frac{P}{2}\frac{L_m}{L_r}\left(\psi_{rd}i_{sq} - \psi_{rq}i_{sd}\right) - T_L\right) \tag{3}$$

The motor torque is expressed by rotor flux magnitude and stator current component, if the rotor can be kept constant as in the case of DC machine, then the torque control is accomplished by controlling the current component [24].

$$\frac{d\omega_r}{dt} = \frac{1}{J}\left(\frac{2}{3}\frac{P}{2}\frac{L_m}{L_r}\left(\psi_r i_{sq}\right) - T_L\right) \tag{4}$$

The two phase *d-q* model of an induction machine rotating at a speed will give the decoupled control concept. The complete motor dynamic equation is obtained by separating the real and imaginary components as:

$$\vec{V}_{sq} = R_s i_{sq} + L_s\frac{di_{sq}}{dt} + L_m\frac{d}{dt}i_{rq} + L_s\omega_e i_{sd} + L_m\omega_e i_{rd} \tag{5}$$

$$\vec{V}_{sd} = R_s i_{sd} + L_s\frac{di_{sd}}{dt} + L_m\frac{d}{dt}i_{rd} - L_s\omega_e i_{sq} - L_m\omega_e i_{rq} \tag{6}$$

$$0 = R_r i_{rd} + L_r\frac{di_{rd}}{dt} + L_m\frac{d}{dt}i_{sd} - L_r\left(\omega_e-\omega_r\right)i_{rq} + L_m\left(\omega_e-\omega_r\right)i_{sq} \tag{7}$$

$$0 = R_r i_{rq} + L_r\frac{di_{rq}}{dt} + L_m\frac{d}{dt}i_{sq} + L_r\left(\omega_e-\omega_r\right)i_{rd} + L_m\left(\omega_e-\omega_r\right)i_{sd} \tag{8}$$

where,

$L_s = L_m(1+\sigma_s)$	: Stator self Inductance
L_m	: Magnetizing Inductance
$L_r = L_m(1+\sigma_r)$	: Rotor self Inductance
R_s	: Stator resistance
R_r	: Rotor resistance
T_d	: Electromagnetic torque
ω	: Angular speed
P	: Number of poles

The induction motor model is often used in vector control algorithms, for this, reference frame may be aligned with the stator flux linkage, rotor flux linkage or the magnetizing space vector. The most accepted reference frame is the frame attached to the rotor flux linkage, this can be achieved by deciding ω_τ to be the speed of rotor and locking the phase of the reference system so that the rotor flux is aligned with the d axis.

The fundamental equations for vector control which allows the induction motor to act like a separately excited DC machine with decoupled control [6]of torque and flux making the induction motor to operate as a high performance four quadrant servo drive [25]. From the voltage loop equation, the magnetizing current dependency on the d component of stator current is obtained as:

$$\frac{d\psi_{rd}}{dt} + R_r i_{rd} = i_{sd} \tag{9}$$

$$i_{mr} = \frac{i_{sd}}{(1+s\tau_r)} \tag{10}$$

where

$$\tau_r = \frac{L_r}{R_r}$$

Slip speed is calculated based on the following equations:

$$\omega_{slip} = \frac{1}{\tau_r}\frac{i_{sq}}{i_{mr}} \tag{11}$$

$$\omega_e = \omega_r + \omega_{slip} \tag{12}$$

$$J\frac{d\omega_r}{dt} = \frac{2}{3}\frac{P}{2}\frac{L_m}{(1+\sigma_r)}i_{mr}i_{sq} - T_L \tag{13}$$

where,

τ_r	: Rotor time constant
i_{mr}	: Rotor magnetizing current component along rotor flux axis
ω_{slip}	: Slip speed
ω_e	: rotor flux speed

ISBN: 978-988-19252-8-2
ISSN: 2078-0958 (Print); ISSN: 2078-0966 (Online)

III. Field Weakeining Control of Induction Machine

Field weakening is made in order to allow operation of variable speed induction motor drives at high speeds. Fig. 2 shows the typical capability curve of induction machine.

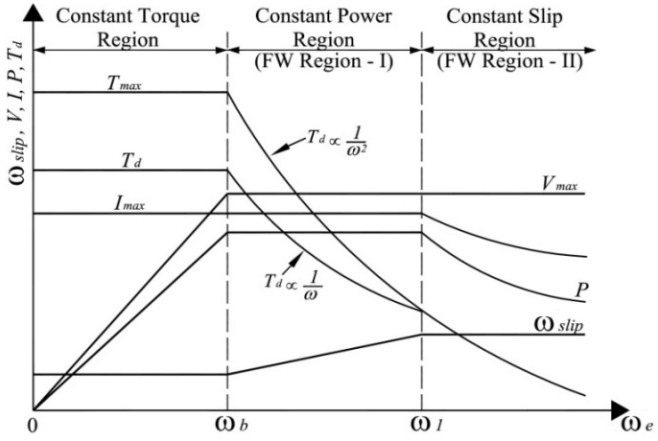

Fig. 2. Typical Capability curve of Induction machine

The voltage cannot be increased over the nominal value, the increase of speed must be done by sacrificing the overall torque produced. The limiting factor of maximum torque capability in field weakening mode of operation is the DC bus voltage. The simplest way of field weakening is to vary stator flux magnitude in inverse proportion to speed known as $1/\omega_r$. The performance of AC machine driven by a three phase SVPWM inverter in the high speed range is limited by the voltage and current rating of electric machine and inverter and the machine thermal rating [26].The stator voltage equation is approximated by neglecting stator resistance effect at higher operating speed as,

$$V_{sd} \approx \omega_e \sigma L_s i_{sq}$$
$$V_{sq} \approx \omega_e L_s i_{sd} \quad (14)$$

The voltage limit boundary is an ellipse and the shape of the ellipse is determined by its eccentricity which depends on the leakage factor of the machine [3]. The maximum phase voltage is decided by the PWM strategy and the *d-q* axis stator voltage should satisfy the following inequality condition, which sensibly influence the motor behaviour and the voltage limit ellipse equation as follows,

$$V_{sd}^{\ 2} + V_{sq}^{\ 2} \le V_{sm}^{\ 2} \quad (15)$$

$$\frac{i_{sd}^{\ 2}}{\left(\frac{V_{sm}}{\omega_e L_s}\right)^2} + \frac{i_{sq}^{\ 2}}{\left(\frac{V_{sm}}{\omega_e L_s'}\right)^2} \le 1 \quad (16)$$

where,

$$L_s' = \sigma L_s$$

The maximum current to the machine is also limited, and the current limit boundary is a circle, whose radius depends only on the current rating, as follows,

$$I_{sd}^{\ 2} + I_{sq}^{\ 2} \le I_{sm}^{\ 2} \quad (17)$$

Speed estimation in the base speed range is based on a constant value of magnetic inductance. In FW region, magnetic inductance L_m varies due to the variation in the degree of main flux saturation. Thus both the reference and adaptive models are to be modified to account the main flux saturation by using the appropriate state space models of a saturated induction machine as explained in [21]. In induction machine, the main flux saturation effects are accurately accounted by means of machine hysterisis magnetizing curve described by the non linearity [27]. The magnetizing flux and magnetizing inductance change to functions of magnetizing current [28].

At a given operating frequency, to satisfy voltage and current constraints, the command current must be inside the common area of a circle and an ellipse. Fig. 3 shows voltage limit boundary, current constraint circle and constant torque locus. In steady state and rotor flux orientation condition, the torque of the field oriented induction machine is expressed as,

$$T_d = \frac{2}{3}\frac{P}{2}\frac{L_m^{\ 2}}{L_r}\left(i_{sd} i_{sq}\right) \quad (18)$$

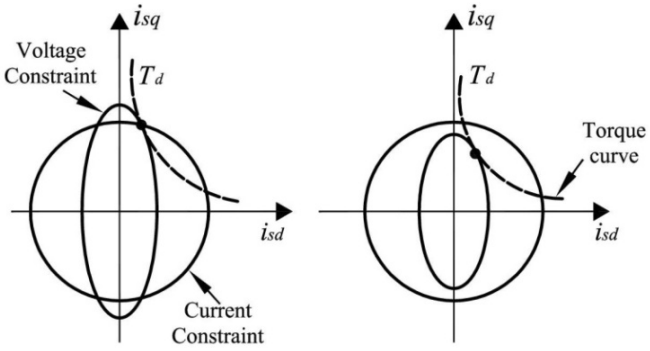

a. FW Region I b. FW Region II

Fig. 3. Voltage constraint ellipse, current constraint circle and torque locus

The operation of the induction motor can be divided into three speed ranges, i) constant electromagnetic torque region ii) constant power speed range iii) constant slip frequency region [12]. In the constant torque region the speed is less than the rated speed and the d axis current is kept constant. In this current limit and the rated flux level determine the operating point to the maximum torque. The base frequency is the angular frequency where the constant torque operation region terminates is given as,

$$\omega_b = \frac{V_{sm}}{L_s}\sqrt{\frac{1}{[\sigma^2(I_{sm}^{\ 2} - i_{sd}^{\ 2}) + i_{sd}^{\ 2}]}} \quad (19)$$

In field weakening region I, the ellipse shrinks as the speed increases and goes beyond its rated speed [17], it is necessary to reduce the rotor flux magnitude, the d axis current is no longer a constant. In this region, the power delivered to the load is nearly constant because the maximum torque is inverse proportion to the mechanical speed, the operation region starts from the base speed and ends at ω_1.

ISBN: 978-988-19252-8-2
ISSN: 2078-0958 (Print); ISSN: 2078-0966 (Online)

$$\omega_1 = \frac{V_{sm}}{L_s I_{sm}} \sqrt{\frac{(1+\sigma^2)}{2\sigma^2}} \tag{20}$$

The characteristic region of the induction machine referred to as flux weakening region II, the operating frequency of the induction machine further increases from ω_1 and the ellipse is encircled by the current constraint circle, the power delivered to the load decreases proportionally with the rotor speed. Fig. 4 shows the flowchart for FW algorithm. In this constant slip frequency region, the maximum torque is inverse proportion to square of the mechanical speed. The maximum q axis current is,

$$i_{sq} = \frac{i_{sd}}{\sigma} \tag{21}$$

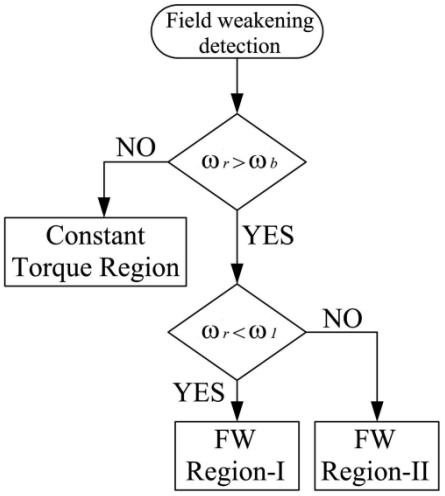

Fig. 4. Flow chart for FW algorithm

IV. SVPWM Based Three Phase Inverter

The principle of SVM is based on the fact that there are only eight possible switching combinations for a three phase inverter to calculate inverter transistor on times. The transition from one switching state to the next involves only two switches in the same inverter leg, when one being switched ON, the other being switched OFF, in order to minimize the device switching loss [29].

Six non-zero vectors (V_1 to V_6), called the active vectors, shape the axis of hexagonal and the angle between any adjacent two non-zero vectors is 60° [30].The tips of these vectors form a regular hexagon. Two of these states (V_0 and V_7) correspond to a short circuit on the output called the zero vectors, while the other six is considered to form stationary vectors in the α-β complex plane [31] as shown in Fig. 5. The reference voltage is generated by two adjacent non-zero vectors and two zero vectors. In linear operation range on times is calculated as follows,

$$T_1 = \frac{V_{ref}}{V_{DC}} \cdot \frac{\sin(\pi/3-\theta)}{\sin(\pi/3)} . T_s$$
$$T_2 = \frac{V_{ref}}{V_{DC}} \cdot \frac{\sin\theta}{\sin(\pi/3)} . T_s \tag{22}$$

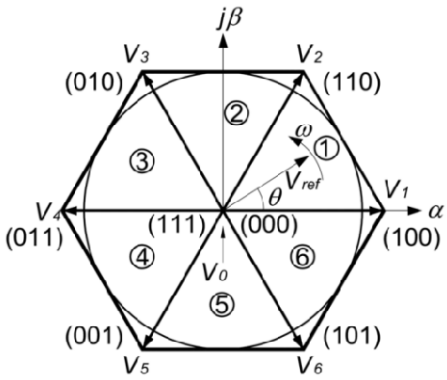

Fig. 5. Space vector hexagon

V. Sliding Mode MRAS Speed Observer

The adaption algorithm for MRAS can be taken into account the overall stability of the system and to ensure that the estimated speed will converge to the desired value with satisfactory dynamic characteristics [32].The adaptive scheme for the MRAS estimator can be designed based on Popov's criteria for hyper stability concept [33], this relate to the stability properties of a class of feedback systems. In MRAS scheme, with two independent machine models,speed estimation is by comparing the output of the reference model with the output of the adaptive (adjustable) model until the error between the two models disappear. Fig. 6 describes the classical rotor flux MRAS with both references and adaptive models for rotor speed estimation. The reference model does not contain the speed to be computed, which represents stator equation and is usually known as voltage model. The reference value of the rotor flux components in the stationary frame are generated from the monitored stator voltage and current components, which are given by [1], [34].

$$p\psi_{r\alpha} = \frac{L_r}{L_m}\left[(v_{s\alpha} - R_s i_{s\alpha}) - \sigma L_s p i_{s\alpha}\right] \tag{23}$$

$$p\psi_{r\beta} = \frac{L_r}{L_m}\left[(v_{s\beta} - R_s i_{s\beta}) - \sigma L_s p i_{s\beta}\right] \tag{24}$$

where,

$$\sigma = 1 - \frac{L_m^{\,2}}{L_s L_r} \tag{25}$$

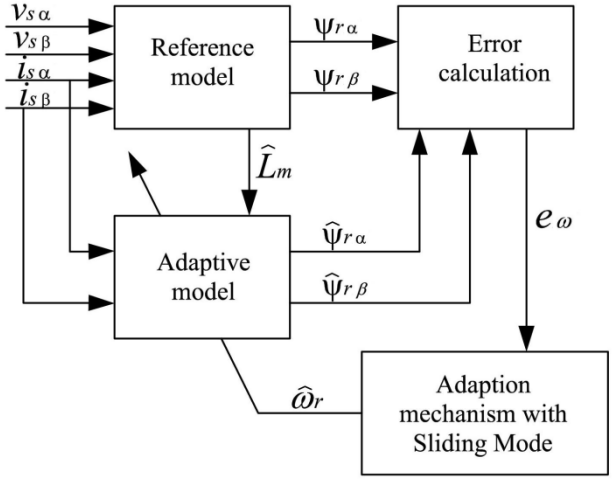

Fig. 6. Bock diagram of modified MRAS-SM speed estimator for FW

ISBN: 978-988-19252-8-2
ISSN: 2078-0958 (Print); ISSN: 2078-0966 (Online)

The adaptive model contains the estimated rotor speed, which represents the rotor equation and is usually known as the current model. The adaptive values of rotor flux components are given by [1], [34]

$$\hat{\psi}_{r\alpha} = \frac{1}{T_r}\int (L_m i_{s\alpha} - \hat{\psi}_{r\alpha} - \hat{\omega}_e T_r \hat{\psi}_{r\beta})dt \quad (26)$$

$$\hat{\psi}_{r\beta} = \frac{1}{T_r}\int (L_m i_{s\beta} - \hat{\psi}_{r\beta} + \hat{\omega}_e T_r \hat{\psi}_{r\alpha})dt \quad (27)$$

$$e_\omega = \psi_{r\beta}\hat{\psi}_{r\alpha} - \psi_{r\alpha}\hat{\psi}_{r\beta} \quad (28)$$

The difference between the two estimated vectors is fed to an adaption mechanism to generate estimated value of rotor speed which is used to tune the adaptive model. The tuning signal, e_ω actuates the rotor speed, which makes the error signal zero. The major problems associated with the classical MRAS speed estimator described above are those related to initial condition and integrator drift which is solved by substituting pure integration with low pass filtering as proposed in [16].Variation in the stator resistance due to temperature changes, significantly affects the accuracy of speed estimation at very low frequencies. However, at high frequencies (FW region) variation of stator resistance has practically no impact on the accuracy of the speed estimation [21].

Sliding mode control is considered to be the appropriate methodology for the robust nonlinear control of induction motor drives due to its order reduction, disturbance rejection, strong robustness and simple implementation by means of power converter [35]. SMC is a control strategy in variable structure system (VSS) having a proper switching logic with high frequency discontinuous control actions depending on the system state, disturbances, and reference inputs. The basic concepts, mathematical approaches and design procedure are explained in [35], [36].

The sliding mode is a control technique to adjust feedback by previously defining surface. In SMC a control law is designed so as to bring the system trajectory on a predefined surface called the sliding surface. Sliding phase is that phase where it slides along the predefined surface to the equilibrium point and reaching phase is the phase before it touches the sliding surface. The system which is to be controlled will be then forced to that surface and the behaviour of the system slides to the desired equilibrium point [37].

In sliding mode controller the system is controlled in such a way that the error in the system states always move towards a sliding surface. The sliding surface is defined with the tracking error of the state and its rate of change as variables. The control input to the system is decided by the distance of the error trajectory from the sliding surface and its rate of convergence. At the intersection of the tracking error trajectory with the sliding surface the sign of the control input must be changed, thus the error trajectory is always forced to move towards the sliding surface. The sliding mode control should be chosen such that the candidate Lyapunov function, V which is a scalar function of S and its derivative satisfies the Lyapunov stability criteria,

$$V(S) = \frac{1}{2}S(x)^2 \quad (29)$$

In Lyapunov theory, if the time derivative of *V(S)* along a system trajectory is negative definite, this will ensure that it constrains the state trajectories to a point towards the sliding surface *S(t)* and once on the surface, the system trajectories remain on the surface until the origin is reached asymptotically. Thus the sliding condition is achieved by the following condition (30) makes the surface an invariant set.

$$\dot{V}(x) \le -\eta|S(x)| \quad (30)$$

where,

η - strictly positive constant on outside of *S(t)*.

The control rule is written as:

$$u(t) = u_{eq}(t) + u_{sw}(t) \quad (31)$$

The sliding mode control should be chosen such that the candidate Lyapunov function, V which is a scalar function of S and its derivative satisfies the Lyapunov stability criteria,

$$\dot{V}(S) = S(x)\dot{S}(x) \quad (32)$$

where, *u(t)* is the control vector, $u_{eq}(t)$ is the equivalent control vector and $u_{sw}(t)$ is the switching vector and must be calculated so that stability condition as per (32) for the selected control is satisfied.

$$u_{sw}(t) = \eta sign(S(x,t)) \quad (33)$$

where,

$$sign(S) = \begin{cases} -1 & for\ S < 0 \\ = 0 & for\ S = 0 \\ +1 & for\ S > 0 \end{cases}$$

The sliding mode control theory is now applied to the rotor flux MRAS scheme for speed estimation by replacing the conventional constant gain PI controller. With reference to dynamic model of induction machine and the speed tuning signal of (28), the time varying sliding surface *S(t)* is constructed as in [38]:

$$S(t) = e_\omega + \int K e_\omega dt = 0 \quad (34)$$

where, K is the switching gain which is strictly positive constant. When the system reaches the sliding surface, the error dynamics at the sliding surface, *S(t) = 0* will be forced to exponentially decay to zero. Thus,

$$\dot{S} = \dot{e}_\omega + K e_\omega = 0 \quad (35)$$

substituting (35) in (32),

$$\dot{V}(S) = S(\dot{e_\omega} + K e_\omega) = S(a + K e_\omega - \hat{\omega}_r b) \quad (36)$$

where,

$$a = \dot{\psi}_{r\beta}\hat{\psi}_{r\alpha} - \dot{\psi}_{r\alpha}\hat{\psi}_{r\beta} + \frac{L_m}{T_r} i_{s\alpha}\psi_{r\beta} - \frac{1}{T_r} i_{r\alpha}\hat{\psi}_{r\alpha}\psi_{r\beta}$$

$$-\frac{L_m}{T_r} i_{s\beta}\psi_{r\alpha} + \frac{1}{T_r}\hat{\psi}_{r\beta}\psi_{r\alpha} \quad (37)$$

$$b = \psi_{r\beta}\hat{\psi}_{r\beta} + \psi_{r\alpha}\hat{\psi}_{r\alpha} \quad (38)$$

ISBN: 978-988-19252-8-2
ISSN: 2078-0958 (Print); ISSN: 2078-0966 (Online)

The time derivative of *V(S)* is negative definite for the following conditions:

$$(a + Ke_{\omega} - \hat{\omega}_r b)\begin{cases} <0 & for\ S>0 \\ =0 & for\ S=0 \\ >0 & for\ S<0 \end{cases} \quad (39)$$

This can be attained when:

$$\hat{\omega}_r = u_{eq} + u_{sw} \quad (40)$$

where,

$$u_{eq} = \frac{a + Ke_{\omega}}{b} \quad (41)$$

$$u_{sw} = \eta.sign(S) \quad (42)$$

The equivalent control defines the control action which keeps the state trajectory on the sliding surface and the switching control depends on the sign of the switching surface and η is the hitting control gain which makes (36) negative definite, whose main purpose is to make the sliding condition viable and the value of η should be large enough to overcome the effect of external disturbance [38], [39]. The controller given in (42) will have chattering near sliding surface due to the presence of sign function. This drastic change is avoided by introducing a boundary layer with width, ϕ [40]. By replacing *sign(s)* with *sat(S/ϕ)*, then (42) becomes,

$$u_{sw} = \eta sat(S/\phi) \quad (43)$$

where,

$$sat(S/\phi) = \begin{cases} sign(S/\phi) & if\ |(S/\phi)| \geq 1 \\ (S/\phi) & if\ |(S/\phi)| < 1 \end{cases} \quad (44)$$

A natural solution to reduce the chattering in the estimated speed is by means of a low-pass filter (LPF) as in (45).

$$u_{sw} = \frac{1}{\mu s + 1} u_{sw} \quad (45)$$

VI. Simulation

To evaluate the proposed MRAS with sliding mode observer to estimate the rotor speed and the overall performance of the drive system, computer simulations have been done using MATLAB/Simulink. The block diagram of the drive system for sensorless vector controlled induction machine is shown in Fig. 7. The induction machine used for the simulation is a 1.5 kW having the motor parameters as given in Table I.

TABLE I
Parameters of Induction Motor

R_s	4.850 Ω
R_r	3.805 Ω
L_s	0.274 H
L_r	0.274 H
L_m	0.258 H
I_L	6.5 A
P	4
J	0.03 Nm
B	0.00334 Nm.s

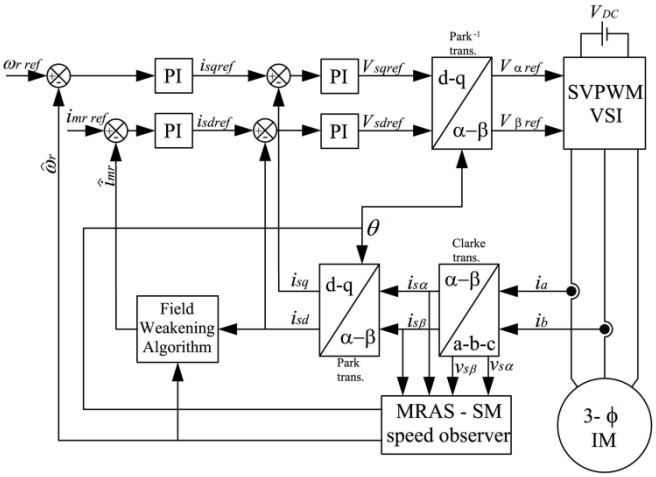

Fig. 7. System configuration of MRAS-SM speed observer for sensorless vector controlled induction machine in FW region

The induction motor is fed by a SVPWM voltage source inverter (VSI). The rotor speed is estimated by MRAS-SM speed observer based on (35) and (40).

VII. Results and Discussion

In the simulation, the motor starts from a standstill state with reference speed 400 rad/sec with no load condition. Fig. 8 shows the rotor speed response with time. The base speed 140 rad/sec is achieved in 0.5 sec and enters to FW region which extends up to 400 rad/sec. From the figure, it is clear that the estimated rotor speed by the proposed MRAS-SM speed observer is close to the actual rotor speed in both base speed and FW region and tracking the reference speed well. Figs.9 and 10 present the transient response of electromagnetic torque as the rotor speed changes from 0 to 400 rad/sec. The motor torque has a high initial value and maintains the rated value of 10.7 N. m. in the base speed region. In the FW region, the motor torque decreases similar to the typical curve as shown in Fig. 2.

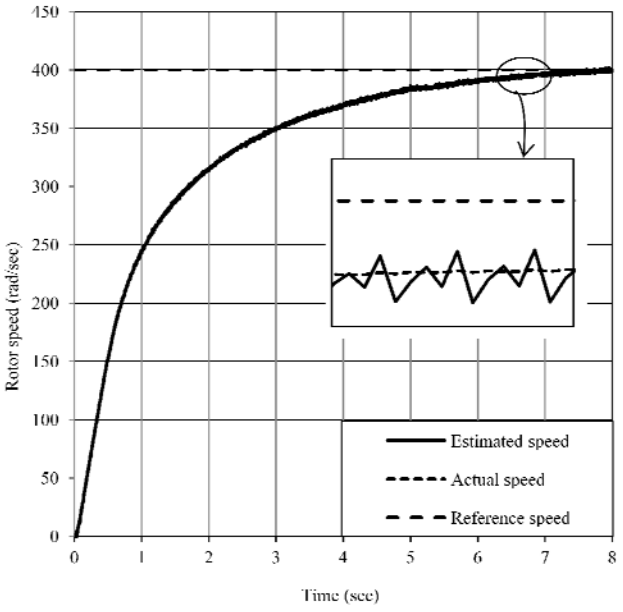

Fig.8. Speed response in FW region

ISBN: 978-988-19252-8-2
ISSN: 2078-0958 (Print); ISSN: 2078-0966 (Online)

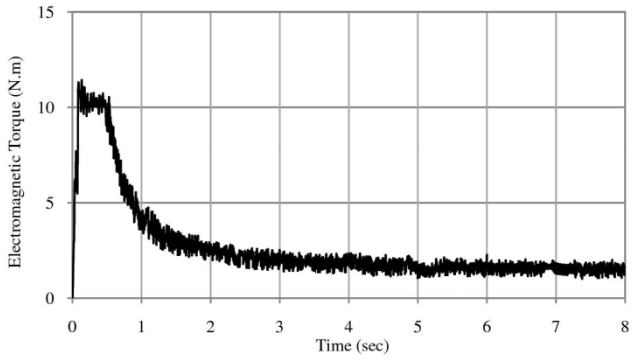

Fig.9. Torque response in FW region

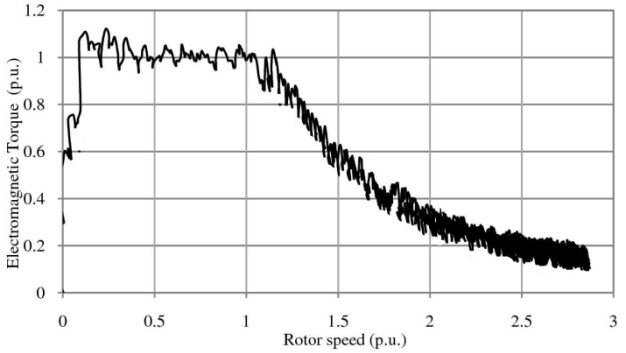

Fig.10. Torque vs. speed in FW region

Fig. 11 shows the variation Power (p.u.) with respect to rotor speed (p.u.). Power maintains constant throughout the FW-I region and then decreases in FW-II region.

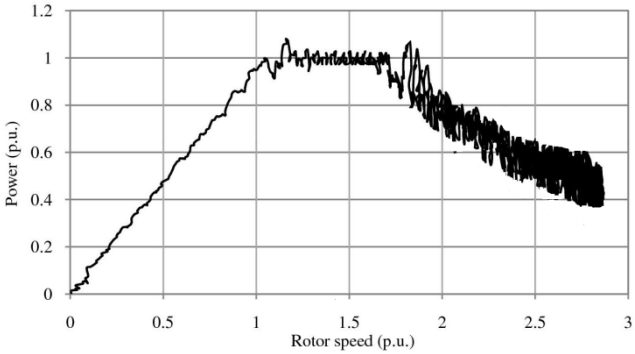

Fig.11. Power vs. speed in FW region

Fig. 12 shows the variation of i_{mr} for rotor speed (p.u.).At starting, i_{mr} = 0.77 p.u. and remains constant in base speed region which drops to 0.25 p.u. when rotor speed = 2.9 p.u. Variations of currents in *d-q* axis, i_{ds} and i_{qs} for both the base speed and FW region are presented in Figs. 13 and 14.

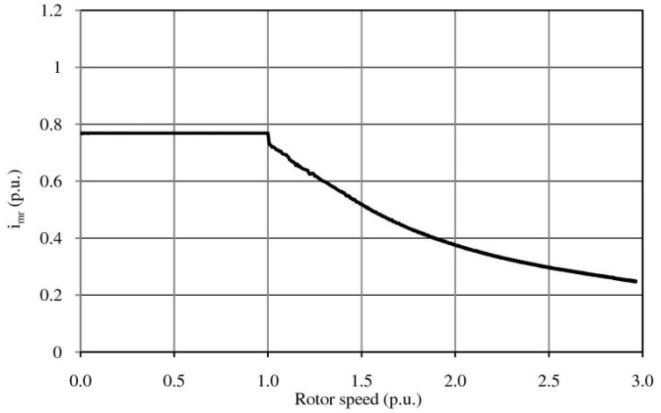

Fig.12. Magnetizing current vs. Rotor speed

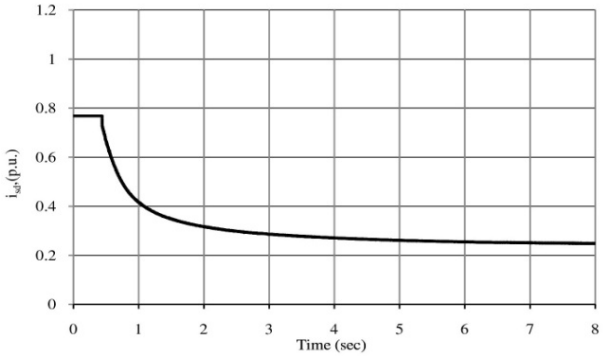

Fig.13. *d* axis currents vs time

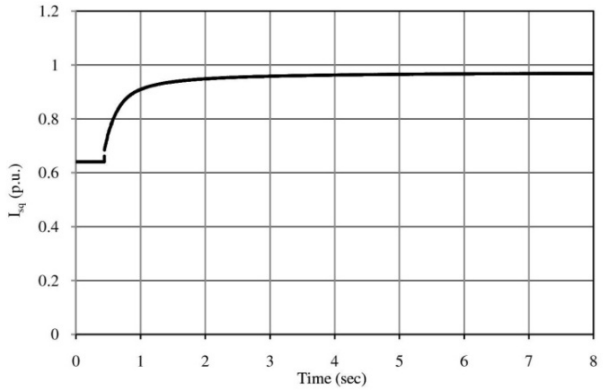

Fig.14. *q* axis currents vs time

Table II presents values of rotor speed, electromagnetic torque and power for i_{mr} = 0.25, 0.45, 0.65 and 0.77.

TABLE II
MOTOR RESPONSE WITH VARIATION OF MAGNETIZING CURRENT

	Magnetizing current i_{mr} (p.u.)			
	0.77	0.65	0.45	0.25
Rotor speed (p.u.)	1.00	1.20	1.70	2.90
Torque (p.u.)	1.00	0.90	0.45	0.15
Power (p.u.)	1.00	1.00	0.90	0.40

By observing all the simulation results, it ensures the ability of proposed MRAS -SM observer to adapt the actual saturation level in the induction machine and hence provide an accurate speed estimation for any operating point in the FW region and works well when the parameters are precisely measured and do not change during operation.

VIII. CONCLUSIONS

In this paper, a novel adaption mechanism using sliding mode control is proposed with MRAS observer in field weakening region for SVPWM fed induction machine. The adaption mechanism is based on Lyapunov theory to ensure stability with fast error dynamics. The performance of the developed MRAS -SM observer has been illustrated in the FW region and the speed and torque responses are analyzed. In this method, the transition speed between base speed region and FW region is smooth, depending upon the voltage and current limits. The speed estimation by the rotor flux MRAS with SM observer has ensured very good accuracy in all ranges of speed control.

ISBN: 978-988-19252-8-2
ISSN: 2078-0958 (Print); ISSN: 2078-0966 (Online)

ACKNOWLEDGMENT

The first author acknowledges support from SPEED-IT Research Fellowship from IT Department of the Government of Kerala.

REFERENCES

[1] H. Abu Rub, Atif Iqbal and Jaroslaw Guzinski, "*High performance control of AC Drives*," NewYork: Wiley, pp. 375-388, 2012.

[2] X. Xu and D. W. Novotny, "Selection of the flux reference for induction machine drives in the field weakening region," *IEEE Trans. Ind. Appl.*, vol. 28, no. 6, pp. 1353-1358, Nov./Dec. 1992.

[3] S. H. Kim and S. K. Sul, "Maximum torque control of an induction machine in the field weakening region," *IEEE Trans. Ind. Appl.*, vol. 31, no. 4, pp. 787-794, Jul./Aug. 1995.

[4] S. H. Song, J. W. Choi and S. K. Sul, "Transient torque maximizing strategy of induction machine in the field weakening region," in *Proc. IEEE PESC*, pp. 1569-1574, May 1998.

[5] F. Briz, A. Diez, M. W. Degner and R. D. Lorenz, "Current and flux regulation in field weakening operation of induction motors," *IEEE Trans. Ind. Appl.*, vol. 37, no. 1, pp. 42-50, Jan./Feb. 2001.

[6] M. H. Shin, D. S. Hyun and S.-B. Cho, "Maximum torque control of stator flux oriented induction machine drive in the field weakening region," *IEEE Trans. Ind. Appl.*, vol. 38, no. 1, pp. 117-122, Jan./Feb. 2002.

[7] H. Grostollen and A. Bunte, "Control of induction motor with orientation on rotor flux or on stator flux in a very wide field weakening region-Experimental results," in *Proc. IEEE ISIE*, pp. 911-916, Jun. 1996.

[8] A. Bunte, H. Grotstollen and P. Krafka, "Field weakening of induction motors in a very wide region with regard to parameter uncertainties," in *Proc. IEEE PESC*, pp. 944-950, Jun. 1996.

[9] S. H. Kim and S. K. Sul, "Voltage control strategy for maximum torque operation of an induction machine in the field weakening region," *IEEE Trans. Ind. Appl.*, vol. 44, no. 4, pp. 512-518, Aug. 1997.

[10] L. Harnefors, K. Pietilanen and L. Gertmar, "Torque-maximizing field weakening control: Design, analysis and parameter selection," *IEEE Trans. Ind. Elect.*, vol. 48, no. 1, pp. 161-168, Feb. 2001.

[11] H. Abu-Rub, H. Schmirgel and J. Holtz, "Sensorless control of induction motors for maximum steady-state torque and fast dynamics at field-weakening," in *Conf. Rec. IEEE IAS Annu. Meeting.*, pp. 96-103, Oct. 2006.

[12] D. Casadei, G. Serra, A. Tani and L. Zarri, "A robust method for field weakening operation of induction motor drive with maximum torque capability," in *Conf. Rec. IEEE IAS*, pp. 111-117, Nov. 2006.

[13] H. Abu-Rub and J. Holtz, "Maximum torque production in rotor field oriented control of an induction motor at filed weakening," in *Proc. IEEE ISIE*, pp. 1159-1164, Jun. 2007.

[14] M. Wlas , H. Abu-Rub and J. Holtz, "Speed sensorless nonlinear control of induction motor in the field weakening region," in *Proc. IEEE EPE-PMEC*, pp. 1084-1089, Sept. 2008.

[15] M. Mengoni, L. Zari, A Tani, G. Serra and D. Casadei, "Stator flux vector control of induction motor drive in the field weakening region," *IEEE Trans. Pow. Electr.*, vol. 23, no. 2, pp. 941-949, Mar. 2008.

[16] D. Casadei, G. Serra, A Tani, and L. Zari, "Field-weakening control schemes for high speed drives based on induction motors," in *Proc. IEEE PESC*, pp. 2159-2166, Jun. 2008.

[17] P. Y. Lin and Y. S. Lai, "Novel voltage trajectory control for field-weakening operation of induction motor drives," *IEEE Trans. Ind. Appl.*, vol. 47, no. 1, pp. 122-127, Jan./Feb. 2011.

[18] Myoung-Ho Shin and Dong-Seok Hyun, "Speed sensorless stator flux oriented control induction machine in the field weakening region," *IEEE Trans. Pow. Elect.*, vol. 18, no. 2, pp. 580-586, Mar. 2003.

[19] P. J. Coussena, A. P. van den Bossche and J. A. Melkebeek, "Magnetizing current control strategies for nonlinear indirect field oriented control," *Proc. IEEE Ind. Appl. Conf.* pp. 538-545, Orlando, F.L., pp. 538-545, Oct. 1995.

[20] E. Levi, M. Sokola and S. M. Vukosavic, "A method for magnetizing curve identification in rotor flux oriented induction machines," *IEEE Trans. Ener. Conv.*, vol. 15, no. 2, pp. 157-162, Jun. 2000.

[21] E. Levi and M. Wang, "A speed estimator for high performance sensorless control of induction motors in the field weakening region," *IEEE Trans. Pow. Elect.*, vol. 17, no. 3, pp. 365-378, May.2002.

[22] A.V. Stancovie, E. L Benedict, J. Vinod and T.A. Lipo, "A novel method for measuring induction machine magnetizing inductance", *IEEE Trans. Ind. Appl.*, vol. 39, no. 5, pp. 1257-1263,Sept./Oct. 2003.

[23] G. K. Nisha, Z. V. Lakaparampil and S. Ushakumari, "Sensorless vector control of SVPWM fed induction machine using MRAS – sliding mode", *in Proc. IEEE ICGT 2012*, pp. 29-36, Dec.2012.

[24] W. Leonhard, "*Control of Electrical Drives*," New York: Springer, pp. 163-180, 1996.

[25] Z. V. Lakaparampil, K. A Fathima and V.T. Ranganathan,"Design modeling simulation and implementation of vector controlled induction motor drive*," in Proc. PEDES*, vol. 2, pp. 862-868, Jan.1996.

[26] Seung-Ki Sul, "*Control of Electric Machine Drive Systems*," New Jersey: Wiley, pp. 255-267, 2011.

[27] P. Vas, *Electrical Machines and Drives: A Space vector Theory Approach.* Oxford: Clarendon Press,1992.

[28] A. B. Ali, A. Khedher, M. F. Mimouni and R. Dhifaoui,"Torque maximization and sensorless control of induction motor in a flux weakening region", *IJSTA*, vol.3, no. 1, pp. 972-985*,* Jul. 2009.

[29] G. K. Nisha, S. Ushakumari and Z. V. Lakaparampil, "Harmonic Elimination of Space Vector Modulated Three Phase Inverter", *in Proc. IMECS 2012,* pp. 1109-1115, Mar. 2012.

[30] H. W. Van der Broeck, H. C. Skudelny and G.V. Stanke," Analysis and realisation of a pulse width modulator based on voltage space vectors", *IEEE Trans. Ind. Appl.*, vol. 24, pp. 142-150, Jan./Feb. 1988.

[31] D. G. Holmes and T. A. Lipo, "Pulse Width Modulation for Power Converters: Principles and Practice," *New Jersey: Wiley* IEEE Press, 2003.

[32] B. K. Bose, "*Modern Power Electronics and AC drives*," Prentice Hall of India Pvt. Limited, New Delhi, pp. 390-392, 2009.

[33] Y. D. Landau, "*Adaptive Control-The Model Referencing Approach*," Marcel Dekker, 1979.

[34] C. Schauder, "Adaptive speed identification for vector control of induction motors without rotational transducers," *IEEE Trans. Ind. Appl.*, vol. 28, no. 5, pp. 1054-1061, Sept./Oct.1992.

[35] A. Derdiyok, "A novel speed estimation algorithm for induction machines," *Elect. Pow. Syst. Resr.,* no. 64, pp. 73-80, Jun. 2003.

[36] V.I. Utkin, "Sliding mode control design principles and applications to electric drives," *IEEE Trans. Ind. Elect.,* vol. 40, no. 1, pp. 23-36, Feb. 1993.

[37] J. J. E. Slotine and W. Li, "*Applied Non Linear Control,*" New Jersey: Prentice Hall, pp. 276-286, 1998.

[38] M. Abid, Y. Ramdani and A. K. Meroufel,"Speed Sliding mode control of sensorless induction machine, "*Elect. Engg.,* vol.57, no.1, pp. 47-51, Apr. 2006.

[39] J. C. Lo and Y. Y. H. Kuo, "Decoupled fuzzy sliding mode control," *IEEE Trans. Fuzzy Syst.,* vol. 6, no.3, pp. 426-435, Aug. 1998.

[40] M. Comanescu and L. Xu, "Sliding mode MRAS speed estimators for sensorless vector control of induction machine", *IEEE Trans. Ind. Elect.,* vol. 53, no. 1, pp. 146-153, Feb. 2006.